Estimation of ground thermal diffusivity using the conjugate gradient method with adjoint problem formulation

Zhanat Karashbayeva, Julien Berger, Helcio R B Orlande, Bolatbek Rysbaiuly

Estimation of ground thermal diffusivity using the conjugate gradient method with adjoint problem formulation

Zhanat Karashbayeva [a, b*], Julien Berger[a], Helcio R.B. Orlande[c], Bolatbek Rysbaiuly[d]

[a] Laboratoire des Sciences de l'Ingénieur pour l'Environnement (LaSIE), UMR 7356 CNRS, La Rochelle Université, CNRS, 17000, La Rochelle, France
[b] Astana IT University, Astana, Kazakhstan
[c] POLI/COPPE, Mechanical Engineering Department, Federal University of Rio de Janeiro
[d] International Information Technology University, Manas Str. 34/1, Almaty, Kazakhstan
*corresponding author, e-mail address : Zhanat.Karashbayeva@univ-lr.fr

Abstract

In the context of better evaluating the energy balance between the ground surface and the urban thermal environment, the ground diffusivity is a crucial parameter. The aim of this paper is to indirectly measure this property of an heterogeneous ground by solving an inverse problem. The conjugate gradient method with adjoint problem formulation was applied to solve the inverse problem with temperature measurements taken at different depths obtained in an experiment reported in the literature. Results show that the inverse problem solution was stable and effective. Estimated values of thermal diffusivity obtained in this works were in accordance with literature values. The reliability of the mathematical model with the estimated thermal diffusivity values was addressed with measurements different from those used for the inverse analysis.

Key words: inverse heat conduction problem; heat equation; thermal diffusivity; conjugate gradient method; urban ground.

1 Introduction

In accordance with the recent statistics, the global urbanization rate is above 50% and it is expected to further increase in the future. The speed and scale of urbanization has a crucial effect on the urban thermal environment. One of the serious issues in terms of global warming are the urban heat islands (UHI). It has several consequences on outside comfort, microclimate and on building energy needs [1–4]. The heat flux from the urban material is one of the reasons for UHI development. Ground heat flux is a key determinant of the temperature of the ground surface and it couples the energy transfer process at the surface with the energy transfer processes in the ground [5–7]. An introduction to the challenges for elaborating an accurate representation of the physical phenomena can be found in [8]. For the physical modelling, the thermal properties of the ground, such as thermal conductivity, volumetric heat capacity, or more globally the thermal diffusivity, are crucial parameters on ground heat flux and energy balances according to [9]. Consequently, knowledge of accurate values of these properties of the ground is highly important.

The thermal diffusivity of ground can be determined by direct measurements on samples, as presented in [10, 11] for instance. However, such measurements are particular to the samples and sometimes destructive. An alternative solution to retrieve the properties is to solve a parameter estimation problem with *in-situ* measurements [12, 13]. It consists of finding the material properties that minimizes the difference between experimental observations obtained by *in-situ* measurements and the model predictions. Several works from the literature focusing on ground diffusivity estimation will be mentioned in the following. Note that most of the approaches are based on one-dimensional heat transfer equation.

One of the first analytical method for the *in-situ* estimation considers the first harmonic of daily waves, as widely discussed in [14]. This amplitude method assumes that the thermal

diffusivity does not depend on depth or time. In addition, the temperature at the upper boundary is described by a sinusoidal function on a daily basis. A modified version of the amplitude method was proposed by [15]. Moreover, the so-called *Arctangent* method [16] was proposed considering two harmonics. Similarly, the *Logarithmic* method was developed by [17] considering four harmonics and in [18] it was used to determine the thermal diffusivity. All these proposed methods assumed a constant diffusivity. Thus, it can be applied to a single layer by considering a homogeneous medium, such as in [19]. However, grounds are naturally heterogeneous and this fact is reflected on their physical properties.

In order to indirectly measure heterogeneous thermal diffusivities, the inverse problem procedures must rely on temperatures measured at different ground locations. Inverse problems based on actual experimental data are in general complicated since solutions are affected by both measurement and model errors. Thus, most of the works devoted to the estimation of heterogeneous ground thermal properties were based on simulated measurements [20–22]. Some studies indeed considered actual measurements such as [23, 24]. In [23] the *Levenberg–Marquardt* method was used to solve the inverse problem. Although the results of the method were accurate, they are limited to laboratory experiments and need to be validated for real field experiments. In [24], the thermal conductivity was considered as dependent on ground types and moisture content. It was assumed three ground layers: top (10 cm), mid or transition (15 cm) and deep (1.35 m). The *Shuffled Complex Evolution* method was used for solving the inverse problem. Authors have determined that the inverse approach based on field data was able to estimate hydraulic and thermal properties. Results for the deep layers were satisfying. However, authors concluded that further investigations were required to gain confidence on the values estimated for the parameters of the top layers. Considering the above cited studies and since the estimation methods of ground thermal diffusivity with real data are poorly studied, more research is still needed on this issue.

The objective of this work is to apply the conjugate gradient method with adjoint problem formulation for estimating the thermal diffusivity of a heterogeneous ground using actual temperature measurements at different depths from the surface [19]. Several works are available in the literature on the use of this method for the solution of inverse problems in heat transfer [20, 25–31]. O.M. Alifanov [28] and his group in the Moscow Aviation Institute have demonstrated the iterative regularization character of the conjugate gradient method with adjoint problem formulation, particularly when the stopping criterion of the iterative procedure is selected based on Morozov's Discrepancy Principle [28, 29].

This paper is structured as follows: Section 2 presents the description of the physical model, the inverse problem method and its algorithm. Section 3 discusses a case study starting from the known parameters of the model. Then, the practical identifiability is demonstrated. Next, results of the parameter estimation problem are presented. Finally, comparison of model predictions with additional data is shown.

2 Methodology

The solution of the inverse problem by using the conjugate gradient method with adjoint problem formulation for estimating the thermal diffusivity of a heterogeneous ground consists of the following basic steps: (i) direct problem formulation that describes the Physical Phenomena; (ii) inverse problem formulation; the solution of auxiliary problems, known as (iii) sensitivity problem and (iv) adjoint problem is required for the minimization of the objective functional; (v) gradient equations; (vi) the iterative procedure; and (vii) computational algorithm. The detailed description of each steps are outlined below.

2.1 Description of Physical Model

The physical problem considers one-dimensional non-stationary heat transfer in grounds defined by the spatial domain $\Omega_x = [0, L]$, where L $[\,\mathsf{m}\,]$ is the ground depth and $\Omega_t = [0, t_f]$ is the time domain, where t_f $[\,\mathsf{s}\,]$ is the time horizon for investigating the phenomena. The physical problem can be formulated as:

$$\rho c_\rho \frac{\partial T}{\partial t} = \frac{\partial}{\partial x}\left(\kappa \frac{\partial T}{\partial x}\right), \tag{1}$$

where ρ $[\,\mathsf{kg}\cdot\mathsf{m}^{-3}\,]$ is the density, c_ρ $[\,\mathsf{J}\cdot\mathsf{kg}^{-1}\cdot\mathsf{K}^{-1}\,]$ is the specific heat, κ $[\,\mathsf{W}\cdot\mathsf{m}^{-1}\cdot\mathsf{K}^{-1}\,]$ is the thermal conductivity, T $[\,\mathsf{K}\,]$ is the temperature of the ground depending on spatial x and time t variables.

The thermal properties vary depending on the ground depth, as shown in Figure 1. A total of N layers is considered for the geometry. It is thus assumed that:

$$\rho \approx \rho_0\,, \qquad c_\rho \approx c_0\,, \qquad \kappa = \kappa(x)\,.$$

that is, with the objective of estimating the thermal diffusivity of each layer, the effective densities and heat capacities of each layer are assumed constant, while the thermal conductivities vary spatially.

Note that the value of thermal diffusivity, α $[\,\mathsf{m}^2\cdot\mathsf{s}^{-1}\,]$, in Section 3 is calculated as:

$$\alpha = \frac{\kappa}{\rho_0\, c_0}.$$

As the heat transfer coefficient and radiation flux are not defined experimentally, considering Robin boundary conditions imply additional unknown parameters (such as the surface heat transfer coefficients, the material absorptivity, etc.) and thus the inverse problem become more complex to solve. Here, to reduce the number of unknown parameters, we propose to use directly the measured data at the surface and at the depth of $x = L$ as Dirichlet boundary conditions:

$$T = T_0(t), \qquad \forall t \in \Omega_t\,, \qquad x = 0\,, \tag{2a}$$

$$T = T_\infty(t), \qquad \forall t \in \Omega_t\,, \qquad x = L\,. \tag{2b}$$

The initial condition is:

$$T = T_{in}(x), \qquad \forall x \in \Omega_x\,, \qquad t = 0\,. \tag{3}$$

The above-mentioned equations (1) to (3) define the direct or forward problem, so that the distribution of temperature $T(x,t)$ can be computed when the physical properties, geometry, number of ground layers, initial and boundary conditions are known.

2.2 Dimensionless formulation

This section presents the dimensionless form of equations (1)–(3). The following dimensionless variables are defined:

$$t^* = \frac{t}{t_{ref}}\,, \qquad x^* = \frac{x}{L}\,,$$

$$U = \frac{T}{T_{ref}}\,, \qquad U_0 = \frac{T_0}{T_{ref}}, \qquad U_\infty = \frac{T_\infty}{T_{ref}} \qquad U_{in} = \frac{T_{in}}{T_{ref}}\,,$$

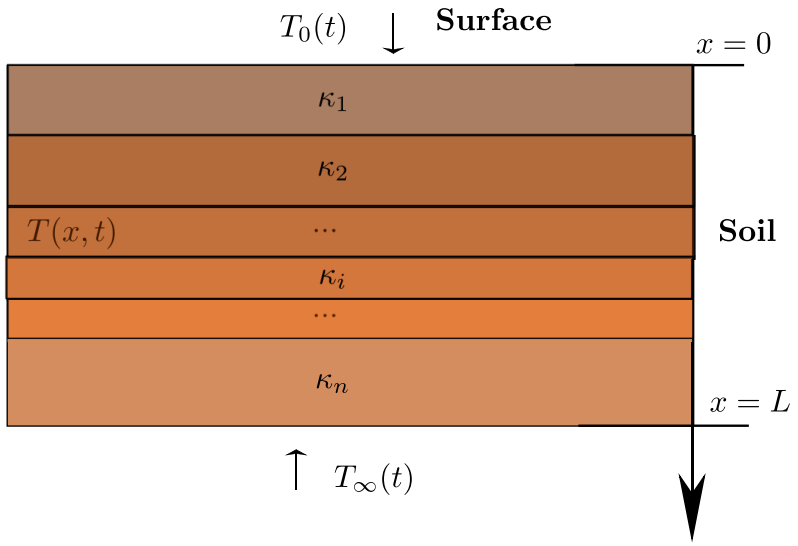

Figure 1. *Illustration of the physical model.*

and the dimensionless coefficients:

$$k \;=\; \frac{\kappa}{\kappa_{ref}}\,, \qquad F_o \;=\; \frac{\kappa_{ref}\cdot t_{ref}}{\rho\cdot c_\rho\cdot L^2}\,.$$

Thus, the heat equation (1) is re-written as:

$$\frac{\partial U}{\partial t^*} \;=\; F_o\,\frac{\partial}{\partial x^*}\left(k(x^*)\frac{\partial U}{\partial x^*}\right)\,, \tag{4}$$

with the DIRICHLET–type boundary conditions:

$$U(0,t^*) \;=\; U_0(t^*)\,, \qquad U(1,t^*) \;=\; U_\infty(t^*)\,, \tag{5}$$

and the initial condition:

$$U(x^*,0) \;=\; U_{in}(x^*)\,. \tag{6}$$

2.3 Inverse Problem

This section presents the methodology to solve the inverse problem in terms of the dimensionless variables defined above. However, for the sake of clarity, the superscript * is omitted. In the inverse problem, the objective is to retrieve the thermal diffusivity of each layer, *i.e.*, estimate the function $k(x)$. For this, the unknown function $k(x)$ is parameterized using a general linear form given by:

$$k(x) \;=\; \sum_{i=1}^{N} k_i\;\phi_i(x), \tag{7}$$

where

$$\phi_i(x) \;=\; \begin{cases} 1\,, & x_i \le x \le x_{i+1}\,, \\ 0\,, & \text{otherwise.} \end{cases}$$

Therefore, the objective of the inverse problem is to estimate N unknown parameters k_i, $i = \{1, \ldots, N\}$, in the vector:

$$\boldsymbol{k} = (k_1, k_2, \ldots k_N).$$

The following objective function is minimized to retrieve the parameter vector $\boldsymbol{k}$, using additional information from the experimental values of the temperature measured with M sensors:

$$S(\boldsymbol{k}) = \sum_{m=1}^{M} \int_0^{t_f} \frac{\Big(U(x_m, t, \boldsymbol{k}) - Y_m(t)\Big)^2}{\sigma_m^2(t)} \, \mathrm{d}t, \tag{8}$$

where $Y_m(t)$ are the measured values of temperature at the M measurement positions x_m, and $U(x_m, t, \boldsymbol{k})$ is the solution of direct problem (4)–(6) evaluated at the same measurement positions x_m with a given $\boldsymbol{k}$. The measurements are supposed to be uncorrelated, with known variance given by the function $\sigma_m^2(t)$ varying in time for the sensor m .

Auxiliary sensitivity and adjoint problems are solved in order to minimize the objective function (8). The solution of the sensitivity problem is the directional derivative of the temperature $U(x,t)$ in the direction of the perturbation of the unknown parameters [28, 31]. The solution of the adjoint problem is a Lagrange multiplier needed for the computation of the gradient equation [28, 31].

2.3.1 Sensitivity Problem

The sensitivity problem can be obtained by assuming that the temperature $U(x,t)$ is perturbed by $\Delta U(x,t)$, when the thermal conductivity $k(x)$ is perturbed by $\Delta k(x)$. By replacing $U(x,t)$ by $U(x,t)+\Delta U(x,t)$ and $k(x)$ by $k(x)+\Delta k(x)$ in the direct problem (4)–(6), and then by subtracting the direct problem from the resulting expressions, we obtain the following sensitivity problem:

$$\frac{\partial \Delta U}{\partial t} = F_o \frac{\partial}{\partial x}\left(k(x)\frac{\partial \Delta U}{\partial x}\right) + F_o \frac{\partial}{\partial x}\left(\Delta k(x)\frac{\partial U}{\partial x}\right), \tag{9a}$$

$$\Delta U(0,t) = 0, \qquad \Delta U(1,t) = 0, \qquad \Delta U(x,0) = 0. \tag{9b}$$

2.3.2 Adjoint Problem

In order to obtain the adjoint problem, we use the following extended objective function:

$$\begin{aligned} S(\boldsymbol{k}) = \sum_{m=1}^{M} \int_0^1 \int_0^{t_f} \frac{\Big(U(x,t,\boldsymbol{k}) - Y_m(t)\Big)^2}{\sigma_m^2(t)} \cdot \delta(x - x_m)\, \mathrm{d}t\, \mathrm{d}x \\ + \int_0^1 \int_0^{t_f} \lambda(x,t)\left(F_o \frac{\partial}{\partial x}\left(k(x)\frac{\partial U}{\partial x}\right) - \frac{\partial U}{\partial t}\right) \mathrm{d}t\, \mathrm{d}x, \end{aligned} \tag{10}$$

where δ is the Dirac delta function, $\lambda(x,t)$ is the Lagrange multiplier. An expression for $\Delta S(\boldsymbol{k})$ of the function $S(\boldsymbol{k})$ can be obtained by perturbing $U(x,t)$ by $\Delta U(x,t)$, and $k(x)$ by $\Delta k(x)$ in equation (10). By replacing $U(x,t)$ by $U(x,t) + \Delta U(x,t)$, $k(x)$ by $k(x) + \Delta k(x)$ and $S(\boldsymbol{k})$ by $S(\boldsymbol{k}) + \Delta S(\boldsymbol{k})$ in (10), subtracting equation (10) from the resulting expression, and neglecting second-order terms, we obtain the following expression:

$$\begin{aligned} \Delta S(\boldsymbol{k}) = \sum_{m=1}^{M} \int_0^1 \int_0^{t_f} 2\, \frac{\Big(U(x,t,\boldsymbol{k}) - Y_m(t)\Big)}{\sigma_m^2(t)} \Delta U(x,t) \cdot \delta(x - x_m)\, \mathrm{d}t\, \mathrm{d}x \\ + \int_0^1 \int_0^{t_f} \lambda(x,t)\left(F_o \frac{\partial}{\partial x}\left(\Delta k(x)\frac{\partial U}{\partial x}\right) + F_o \frac{\partial}{\partial x}\left(k(x)\frac{\partial \Delta U}{\partial x}\right) - \frac{\partial \Delta U}{\partial t}\right) \mathrm{d}t\, \mathrm{d}x, \end{aligned} \tag{11}$$

The second integral on the right-hand side of equation (11) is simplified with integration by parts and by utilizing the boundary and initial conditions of the sensitivity problem. The following expression results:

$$\Delta S(\boldsymbol{k}) = \int_0^1 \int_0^{t_f} \left(\frac{\partial \lambda}{\partial t} + F_o \frac{\partial}{\partial x}\left(k(x) \frac{\partial \lambda}{\partial x} \right) + 2 \sum_{m=1}^{M} \frac{U(x,t,\boldsymbol{k}) - Y_m(t)}{\sigma_m^2(t)} \cdot \delta(x - x_m) \right) \Delta U \, \mathrm{d}t \, \mathrm{d}x + \int_0^{t_f} \lambda \, F_o \, \Delta k(x) \, \frac{\partial U}{\partial x} \Big|_{x=0}^{1} \mathrm{d}t - \int_0^1 \lambda \, \Delta U \Big|_{t=tf} \mathrm{d}x - \int_0^1 \int_0^{t_f} \Delta k(x) \, F_o \frac{\partial \lambda}{\partial x} \frac{\partial U}{\partial x} \, \mathrm{d}t \, \mathrm{d}x. \tag{12}$$

The boundary value problem for the Lagrange multiplier $\lambda(x,t)$ is obtained by allowing the first three integral terms on the right-hand side of (12) to vanish. Thus, the following adjoint problem results:

$$\frac{\partial \lambda}{\partial t} + F_o \frac{\partial}{\partial x}\left(k(x) \frac{\partial \lambda}{\partial x} \right) + 2 \sum_{m=1}^{M} \frac{U(x,t,\boldsymbol{k}) - Y_m(t)}{\sigma_m^2(t)} \cdot \delta(x - x_m) = 0, \tag{13a}$$

$$\lambda(0,t) = 0, \quad \lambda(1,t) = 0, \quad \lambda(x,t_f) = 0. \tag{13b}$$

2.3.3 Gradient Equations

In the limiting process used to obtain the adjoint problem (13), the following integral term remains on the right-hand side of equation (12):

$$\Delta S(\boldsymbol{k}) = - \int_0^1 \int_0^{t_f} F_o \frac{\partial \lambda}{\partial x} \frac{\partial U}{\partial x} \, \mathrm{d}t \Delta k(x) \, \mathrm{d}x.$$

By definition, the directional derivative of $S(\boldsymbol{k})$ in the direction of the vector Δk is given by the scalar product of the gradient vector $\boldsymbol{\nabla} S(\boldsymbol{k})$ and the direction $\Delta k(x)$. By using this definition and the above equation, the following expression is obtained for the gradient direction:

$$\boldsymbol{\nabla} S(\boldsymbol{k}) = - \int_0^{t_f} F_o \frac{\partial \lambda}{\partial x} \frac{\partial U}{\partial x} \, \mathrm{d}t, \tag{14}$$

2.3.4 The iterative procedure

The iterative procedure is now written by taking into account the parameterization of the function $k(x)$ in terms of constant by parts basis functions (equation 7). Starting from an initial guess $\boldsymbol{k}^0$, the iterative procedure for the estimation of the unknown vector at iteration $n+1$ is [13, 31]:

$$\boldsymbol{k}^{n+1} = \boldsymbol{k}^n + \beta^n \boldsymbol{\alpha^n}, \tag{15}$$

where

$$\boldsymbol{\alpha^n} = -\boldsymbol{\nabla} S^n + \gamma^n \boldsymbol{\alpha^{n-1}}, \tag{16}$$

and

$$\beta^n = \frac{\displaystyle\sum_{m=1}^{M} \int_0^{t_f} \frac{[Y_m(t) - U(x_m,t,\boldsymbol{k^n})]}{\sigma_m^2(t)} \Delta U(x_m,t,\boldsymbol{\alpha^n}) \, \mathrm{d}t}{\displaystyle\sum_{m=1}^{M} \int_0^{t_f} \frac{[\Delta U(x_m,t,\boldsymbol{\alpha^n})]^2}{\sigma_m^2(t)} \, \mathrm{d}t}, \tag{17}$$

where $\Delta U(x_m,t,\boldsymbol{\alpha^n})$ is the solution of the sensitivity problem (9) by making $\Delta \boldsymbol{k^n} = \boldsymbol{\alpha^n}$.

By using Polak–Ribiere's version [32] of the conjugate gradient method, the conjugation coefficient is given by:

$$\gamma^n = \frac{\int_0^1 \boldsymbol{\nabla} S^n [\boldsymbol{\nabla} S^n - \boldsymbol{\nabla} S^{n-1}] \, \mathrm{d}x}{\int_0^1 [\boldsymbol{\nabla} S^{n-1}]^2 \, \mathrm{d}x}, \tag{18}$$

with $\gamma^0 = 0$ for $n = 0$. The iterative procedure is applied until a stopping criterion is satisfied. In this work, the following stopping criteria proposed by Dennis and Schnabel [33] was used:

$$\|\boldsymbol{k}^{n+1} - \boldsymbol{k}^n\| < \varepsilon_1, \tag{19}$$

and

$$S(\boldsymbol{k}^n) < \varepsilon_2, \tag{20}$$

where ε_1 is user-defined tolerance and $\| \cdot \|$ is the Euclidean norm. The first criterion (19) evaluates the change in the unknown parameters between two iterations. The second criterion (20) assess the objective function. The tolerance ε_2 is set using Morozov's discrepancy principle [13, 28, 29, 31], considering the standard deviation $\sigma_m(t)$ of the measurements as *a priori* known. Thus, the tolerance ε_2 is obtained from (8), by assuming:

$$|\, U(x_m, t, \boldsymbol{k}) - Y_m(t) \,| \approx \sigma_m(t),$$

and thus $\varepsilon_2 = M t_f$.

2.3.5 The Algorithm

The computational algorithm of the conjugate gradient method with adjoint problem formulation for the estimation of the unknown parameter vector $\boldsymbol{k}$ can be given by the following steps.

Algorithm 1 Algorithm for the conjugate gradient method with adjoint problem.

Require: $\boldsymbol{k}^0$ (initial guess), $\boldsymbol{Y}$ (measured temperatures)
Ensure: $\boldsymbol{k}^{est}$ (estimated value)

1: Set $n = 0$ and k^0
2: **while** $\|\boldsymbol{k}^{n+1} - \boldsymbol{k}^n\| > \varepsilon_1$ or $S(\boldsymbol{k}^{n+1}) > \varepsilon_2$ **do**
3: Compute the direct problem (4)–(6) for given $\boldsymbol{k}^n$
4: Solve the adjoint problem (13)
5: Compute the gradient vector $\boldsymbol{\nabla} S(\boldsymbol{k})$ from Eq. (14)
6: Compute the conjugation coefficients γ^n, with $\gamma^0 = 0$ from Eq. (18)
7: Compute the direction of descent $\boldsymbol{\alpha}^n$ from Eq. (16)
8: By setting $\triangle \boldsymbol{k}^n = \boldsymbol{\alpha}^n$, compute sensitivity problem (9)
9: Compute the search step size β^n from Eq. (17)
10: Compute the new estimate $\boldsymbol{k}^{n+1}$ from Eq. (15)
11: Evaluate the stopping criteria with Eqs. (19) and (20)
12: $n = n + 1$
13: **end while**

3 Case study

3.1 Description

The objective is to estimate the thermal diffusivity of the different layers of the ground. In the first case examined here, the total depth is $L = 75$ cm. The experimental data were provided

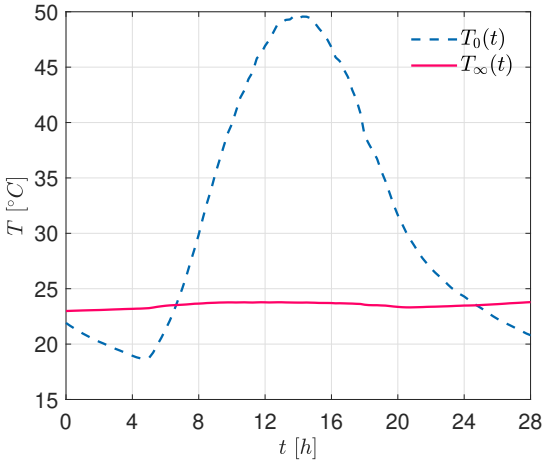

Figure 2. *Time variation of the boundary conditions.*

by [19], from experiments at a parking lot located within the IFSTTAR Institute in Bouguenais, France. The parking lot structure was composed of 5 cm thick layer of asphalt concrete pavement, and a ballast layer under it. Thermocouples were installed to measure the temperature at different ground depths. The measurements at the surface $x = 0$ and at the bottom $x = L$ were used as prescribed temperature boundary conditions for the direct problem (2). Their time variations given as $T_0(t)$ and $T_\infty(t)$ are shown in Figure 2. The $M = 11$ sensors were positioned at $x_m \in \{1, 2, 3, 4, 5, 6, 10, 15, 24, 34, 50\}\ \mathsf{cm}$. Regarding the initial condition, it was obtained by interpolating the values of temperatures at each measurement positions at $t = 0$.

In [19] the ground thermal properties were not measured directly during the experiments. According to the authors, the first layer characteristics were obtained using the temperature measurements at $x = 0\ \mathsf{cm}$ and $x = 1.5\ \mathsf{cm}$ with the amplitude method [34]. The obtained value of the thermal diffusivity, considered as *a priori* information in our work, was $\alpha_{apr} = 1.16 \cdot 10^{-6}\ \mathsf{m}^2 \cdot \mathsf{s}^{-1}$. Note that it has been determined as a constant diffusion coefficient for the first 24 cm of the ground. The following mean values for density and specific heat of the dry asphalt concrete were used $\rho_0 = 2050\ \mathsf{kg} \cdot \mathsf{m}^{-3}$ and $c_0 = 920\ \mathsf{J} \cdot \mathsf{kg}^{-1} \cdot \mathsf{K}^{-1}$, taken from [35].

The initial experiments from [19] were done during 144 h (on June 6 - 12, 2004) in the parking lot of 2500 m^2 flat bare asphalt square. During the whole measurement period, only one natural rain was observed on June 10, and short drizzles on June 8 and 9. The sprinkler system to simulate rain events was adjusted previously (on June 3 and 4), so that all the water fell within the instrumented squared area. Then, starting from June 7 - 11 two simulated rain events were performed each day at different times after the asphalt had completely dried out. They lasted from 20 to 40 min. Conditions on the other days were sunny with cumulus clouds. June 6 was a clear sky day. Since in our model, the phase change of moisture was not taken into account, the estimation procedure was carried out up to $t_f = 28\ \mathsf{h}$ (just before the first rain event). The reliability of the model with estimated parameters will be evaluated including the remaining period, *i.e.*, for times in the interval $[28, 144]\ \mathsf{h}$.

The total uncertainty for each measured temperature at the point x_m was computed by the following formula [36] :

$$\sigma_m = \sqrt{\sigma_{meas}^2 + \sigma_{pos}^2}\,, \qquad \forall m \in \{1, \ldots, M\}\,, \tag{21}$$

where $\sigma_{meas} = 0.1\ °\mathsf{C}$ is the sensor measurement uncertainty and σ_{pos} is the sensor location uncertainty, which is given by following formula:

$$\sigma_{pos} = \left.\frac{\partial T}{\partial x}\right|_{x\,=\,x_m} \cdot \delta_x\,, \tag{22}$$

where $\delta_x = 0.01\ \mathsf{m}$ is the position uncertainty and $\dfrac{\partial T}{\partial x}$ is obtained at the sensor locations using the numerical model. The quantity σ_m varied in time. Note that to solve the parameter estimation problem, the values of position uncertainty σ_{pos} was obtained using α_{apr}. The Figures 6, 7 and 8 exhibit the total uncertainty interval in gray color given by the the standard deviation. Here, experimental errors as sensor measurement and position uncertainties, are assumed as independent and normally distributed.

3.2 Practical identifiability

It is important to analyze the sensitivity coefficients before attempting to solve the parameter estimation problem, in order to evaluate the identifiability of the unknowns. Different approaches exist for the computation of sensitivity coefficients. In our case, the central finite-difference approximation was used, that is,

$$X_{p_{ij}} \approx \frac{T_i(k_1\,, k_2\,, \ldots\,, k_j + \varepsilon k_j\,, \ldots\,, k_N) - T_i(k_1\,, k_2\,, \ldots\,, k_j - \varepsilon k_j\,, \ldots\,, k_N)}{2\,\Delta k} k_j\,,$$

where $\Delta k = 10^{-2}$.

The sensitivity coefficients were obtained using known model parameters ($\kappa = 2\,.19\,\mathsf{W}\cdot\mathsf{m}^{-1}\cdot\mathsf{K}^{-1}$ using thermal diffusivity from [19] given ρ_0 and c_0), for each 11 sensor locations. Figures 3(a) - 3(d) present the time-dependent variations of the sensitivity coefficients at each sensor location. The sensitivity of the parameter k is larger for the sensors located far from the boundaries because of the DIRICHLET-type boundary condition of the model. The temperature being prescribed, the diffusivity is less influenced near the boundaries. We can conclude that the measurements are more sensitive to the parameters in the middle of the domain. Moreover, as in the middle of the domain a sensitivity coefficient has larger magnitudes, we can identify the parameter with better precision [37].

3.3 Results of the Parameter Estimation Problem

The inverse problem was solved using the conjugate gradient method with adjoint problem formulation presented in Section 2.3.5. Numerical solutions of the forward, sentivity and adjoint problems were obtained using the DUFORT–FRANKEL scheme [38]. The dimensionless space and time discretizations used were $\Delta x = 10^{-2}$ and $\Delta t = 10^{-4}$, respectively. The estimated thermal diffusivity was found from:

$$\alpha_{est} \;=\; \frac{\kappa_{est}}{\rho_0\, c_0}.$$

The conjugate gradient method is known to be sensitive to the initial guess used in the iterative procedure. Thus, different initial guesses were considered to solve the parameter estimation problem, as summarized in Table 2. In the first case, the thermal diffusivity used as initial guess is constant over the whole domain. The constant is taken around the *a priori* thermal diffusivity obtained from the investigations carried out in [19]. Preliminary testes, obtained with the constant initial guesses of cases $\alpha_{in,0}$ to $\alpha_{in,4}$, all resulted in linear variations of the thermal diffusivity with the ground depth. Therefore, new initial guesses were tested, with a linear decrease of the thermal diffusivity, in cases $\alpha_{in,5}$ to $\alpha_{in,8}$. The values used in these linear variations were obtained from the thermal diffusivity obtained in case $\alpha_{in,3}$, which resulted in the least value of the objective function with constant initial guess.

Two stopping criteria were used for the iterative procedure to solve the parameter estimation problem. As shown in Figures 4(a) and 4(b) the iterative process was stopped after reaching the tolerance $\varepsilon_1 = 10^{-5}$, given by the first stopping criterion (19). It should be noted that the value of tolerance ($\varepsilon_2 = 308$) given by the second stopping criterion (20) was not reached for all the initial guesses as shown in Figure 4(c) and Figure 4(d). Thus the estimated results did not

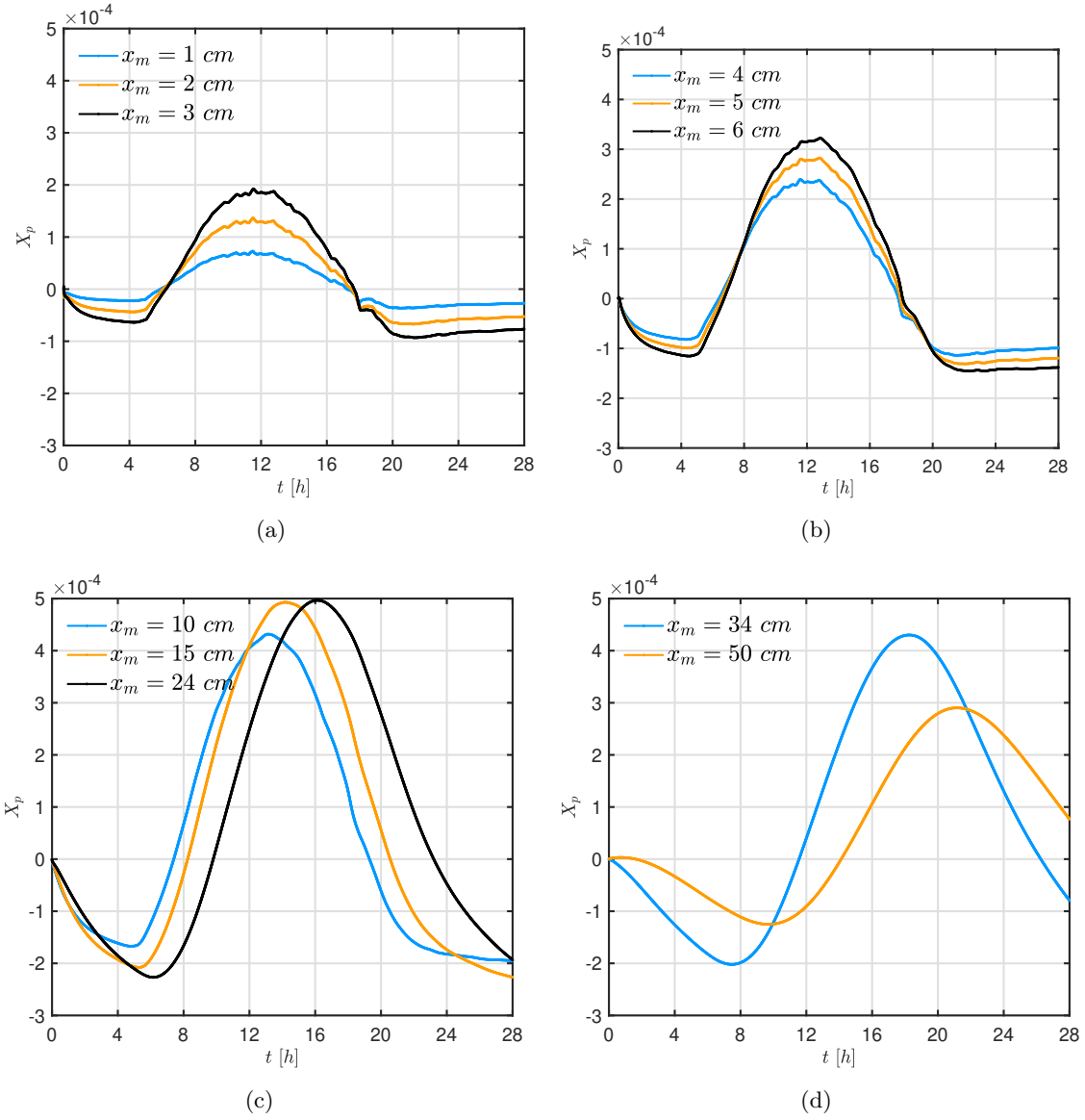

Figure 3. *Sensitivity coefficients for a sensor at:* (a) $x_m = 1,\ 2,\ 3$ cm, (b) $x_m = 4,\ 5,\ 6$ cm, (c) $x_m = 10,\ 15,\ 24$ cm, (d) $x_m = 34,\ 50$ cm.

satisfy the discrepancy principle, probably because the standard deviations of the measurements are not exactly known from a calibration procedure.

Table 2 provides the number of iterations needed for the estimation procedure. It ranges between 8 and 21 iterations. Thus, the algorithm converges fast and the computational time to solve the inverse problem is around 3 minutes. The CPU time has been calculated, using Matlab platform on a computer with Intel(R) Core(TM) i9-10900 CPU @ 2.80GHz and 32 GB of RAM.

The estimated diffusivity is presented in Figures 4(e) and 4(f) for the constant and linearly decreasing initial guesses, respectively. The results obtained with both initial guesses are consistent and exhibit a higher diffusivity for the first 15 cm and then a decreasing diffusivitiy for deeper layers. As shown in from Figure 4(c) and Figure 4(d), the lowest value of the objective function corresponds to the initial guess $\alpha_{in,5}$ (see Table 1). Thus, the estimated values of the thermal diffusivities obtained with the initial guess $\alpha_{in,5}$ were used for the results presented below. The Table 2 shows range of the estimated thermal diffusivity.

The thermal diffusivity was estimated along the ground depths obtained with different num-

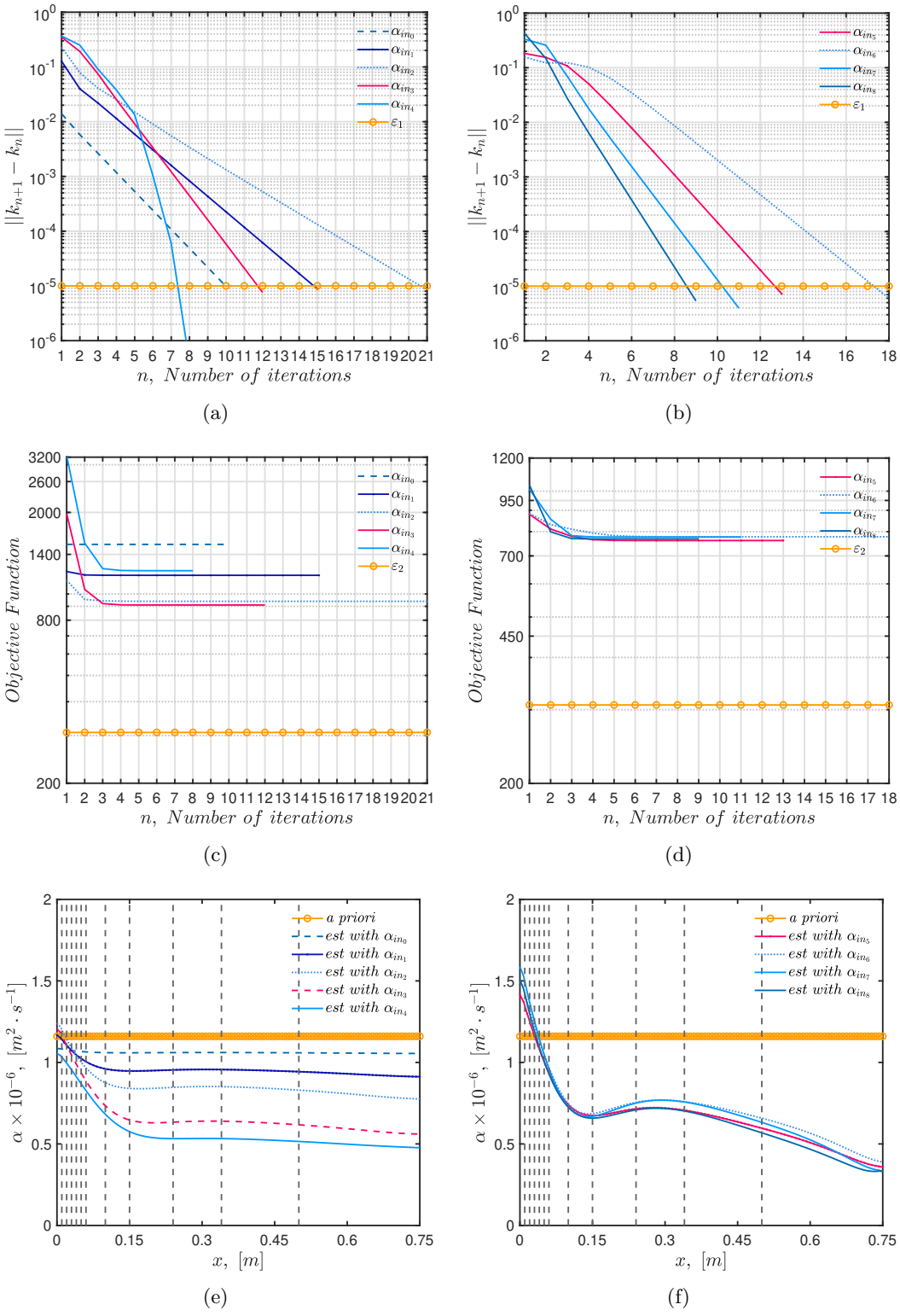

Figure 4. *Variation of the change in the unknown parameters between two iterations:* (a) *constant initial guess,* (b) *space varying initial guess. Variation of the objective function with the algorithm's iterations:* (c) *constant initial guess,* (d) *space varying initial guess. Spatial variation of the a priori known and estimated heat diffusivity with:* (e) *constant initial guess,* (f) *space varying initial guess.*

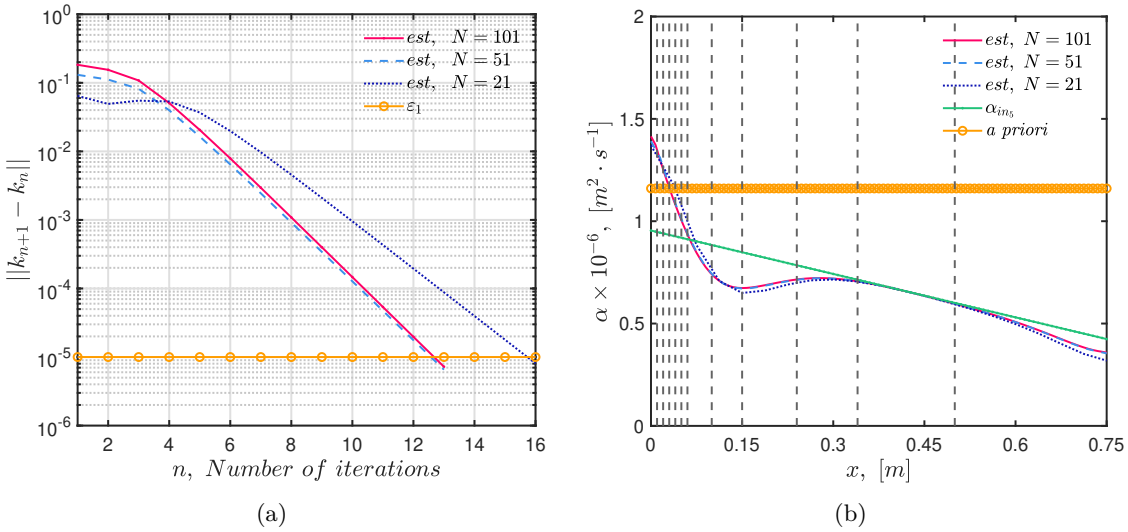

Figure 5. (a) *Variation of the change in the unknown parameters between two iterations.* (b) *Spatial variation of the a priori known and estimated heat diffusion coefficients according to the number of layers* N.

Table 1. *Initial guess and number of iterations to solve the parameter estimation problem.*

	Initial guess, $\mathsf{mm}^2\,.\,\mathsf{s}^{-1}$	*N iterations*	*Objective Function*
α_{apr}	1.16	−−	−−
$\alpha_{in,0}$	1.06	10	1524.20
$\alpha_{in,1}$	0.95	15	1171.77
$\alpha_{in,2}$	0.85	21	939.29
$\alpha_{in,3}$	0.64	12	910.21
$\alpha_{in,4}$	0.53	8	1218.71
$\alpha_{in,5}$	$0.95 - 0.71x$	13	761.85
$\alpha_{in,6}$	$0.95 - 0.56x$	18	777.84
$\alpha_{in,7}$	$1.06 - 0.85x$	11	776.80
$\alpha_{in,8}$	$1.06 - 0.99x$	9	768.63

Table 2. *Estimated thermal diffusivity.*

Material	depth of the ground, x [cm]	Literature α, $[\mathsf{mm}^2\,.\,\mathsf{s}^{-1}]$	α_{est}, $[\mathsf{mm}^2\,.\,\mathsf{s}^{-1}]$
dry asphaltic pavement	$0-5$	$1.15-1.41$ [39]	$1.10-1.41$
different types of soil	>5	$0.138-1.72$ [35, 40]	$0.36-1.04$

bers of layers $N \in \{\,101\,,\,51\,,\,21\,\}$, with layer thicknesses of $\{\,0.75\,,\,1.5\,,\,3.75\,\}$ cm, respectively. Figure 5(a) shows the number of iterations needed for stopping iterative process: 13 iterations were needed for $N = 101$ and $N = 51$, whereas 16 iterations were required for $N = 21$. From Figure 5(b) it can be noticed that the spatial distribution of α_{est} does not significantly vary with N. We can also notice that the thermal diffusivity coefficient estimated here differs from

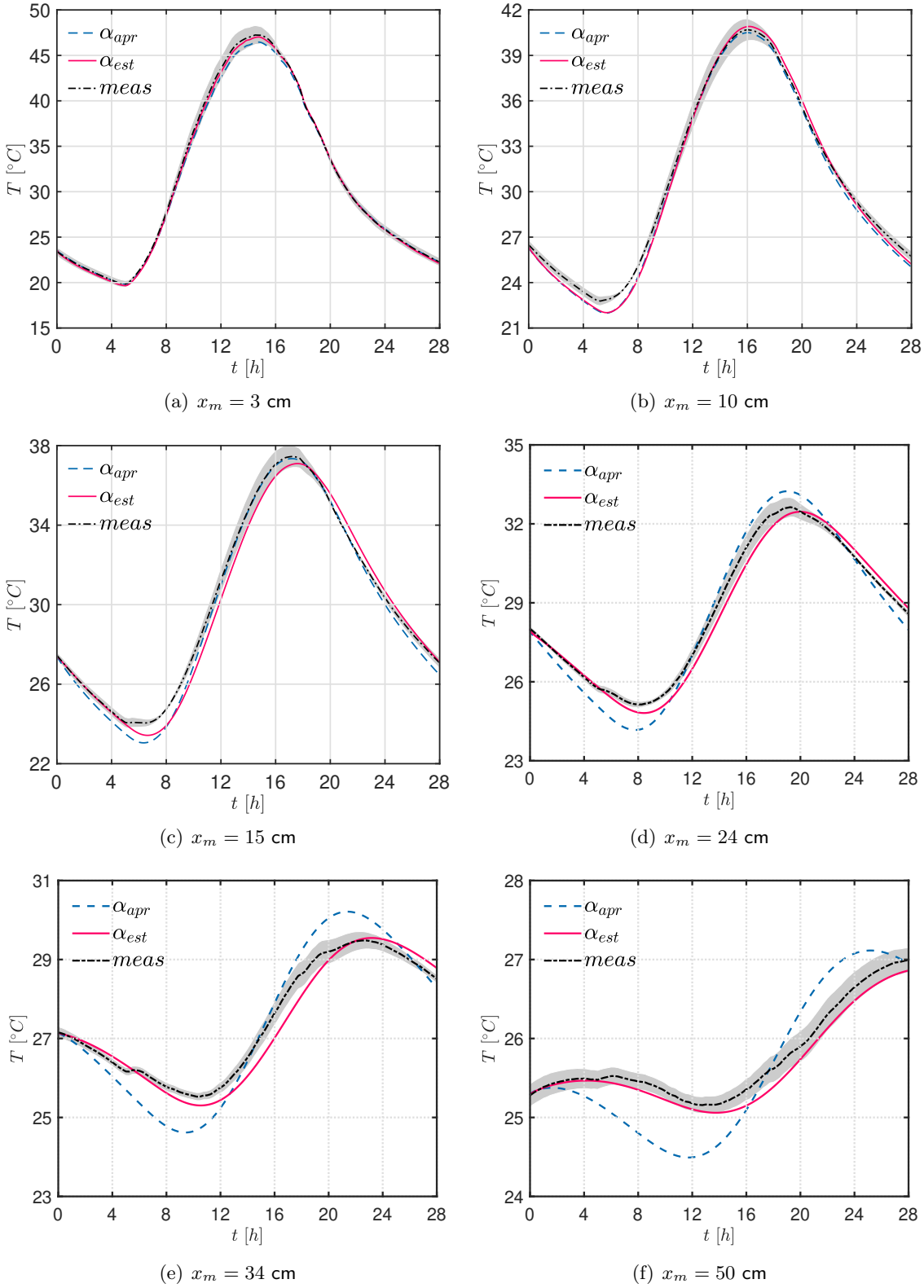

(a) $x_m = 3$ cm (b) $x_m = 10$ cm

(c) $x_m = 15$ cm (d) $x_m = 24$ cm

(e) $x_m = 34$ cm (f) $x_m = 50$ cm

Figure 6. *Computed, a priori and measured values of temperature at several sensor locations.*

the estimations of [19], denoted as *a priori* in Figure 5(b). However, our estimates were within the range of values reported in the literature. For the asphalt layer ($x \in [0, 5]$ cm), the diffusivity reported in [39, 41] is within $[0.44, 1.44]$ $\mathrm{mm}^2 . \mathrm{s}^{-1}$. Regarding the soil ($x > 5$ cm), the diffusivity values were between 0.138 [35] and 1.72 $\mathrm{mm}^2 . \mathrm{s}^{-1}$ [40].

After the estimation procedure, the direct problem was solved with the estimated values of the thermal diffusivities, as well as with the *a priori* known parameter. The corresponding temperatures computed at six measurement positions and the respective measurements are

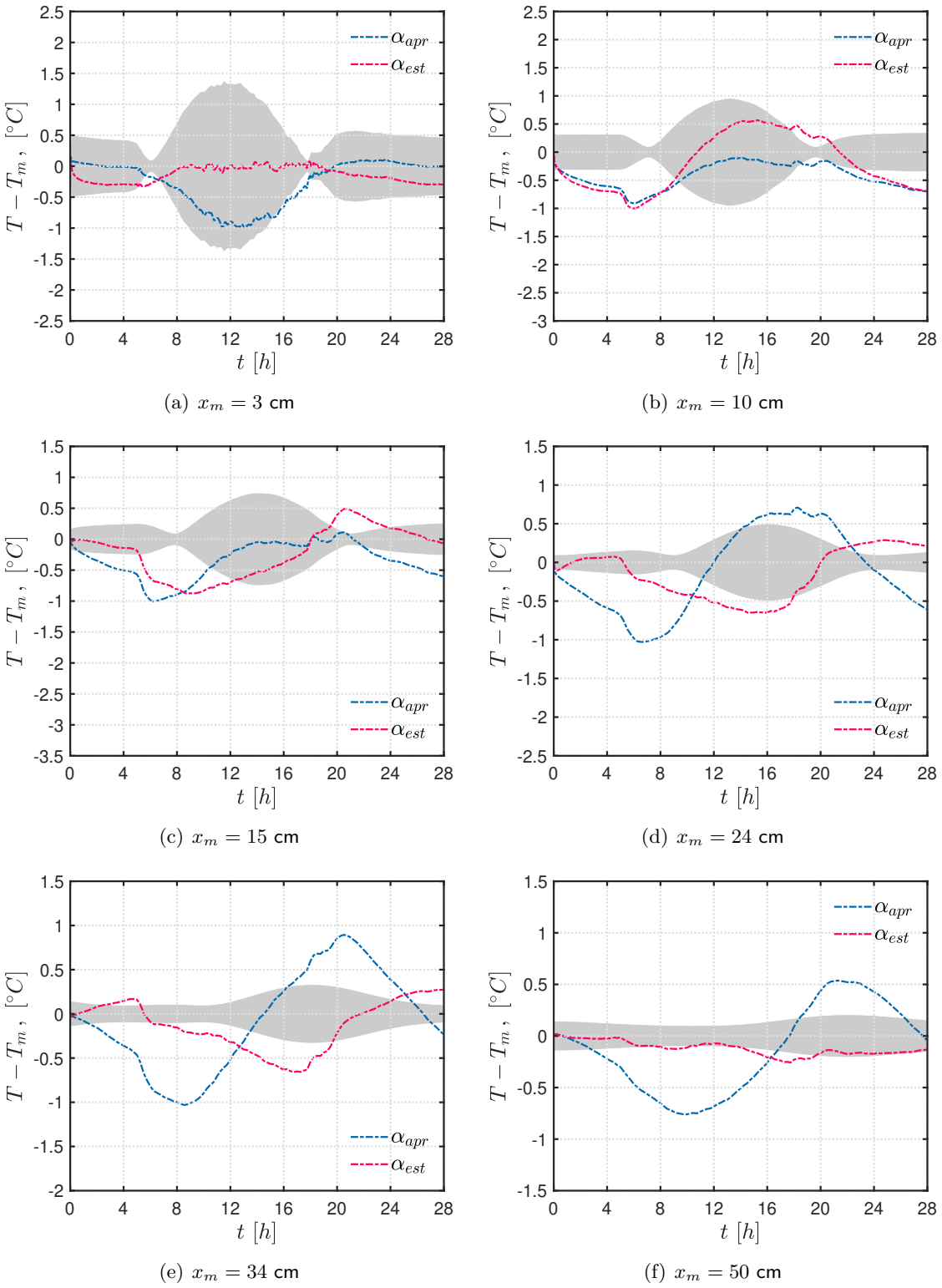

(a) $x_m = 3$ cm (b) $x_m = 10$ cm

(c) $x_m = 15$ cm (d) $x_m = 24$ cm

(e) $x_m = 34$ cm (f) $x_m = 50$ cm

Figure 7. *Difference between computed and measured temperature values at sensor locations.*

compared in Figures 6(a) - 6(f). These figures reveal that the temperatures computed with the thermal diffusivities after the solution of the inverse problem agree with the measurements at least as well as with the temperatures computed with the *a priori* known parameter. However, with the solution of the inverse problem the agreement between temperatures computed with

the estimated thermal diffusivities and measurements has significantly improved for positions $x_m = 3$, 24, 34 and 50 cm. Similar conclusions appear from the analysis of Figures 7(a) - 7(f), which present the temperature residuals at the same measurement positions of Figures 6(a) - 6(f). The residuals are defined by the differences between measurements and temperatures computed with estimated thermal diffusivities. Note that all residuals would be within the standard deviations of the measurements (gray area in the figures) if the discrepancy principle is verified, which tends to be the case at $x_m = \{3, 50\}$ cm. For the other sensors, some local discrepancies appear probably because of other uncertainties not accounted for in the mathematical model and in the solution of the inverse problem. However, the residuals are still centered around zero and quite small, that is, less than 1 $^\circ C$.

Moreover, the Table 3 represents the mathematical analysis between the measured and computed values of the temperature with estimations and *a priori* known values at each measurement point. The Root mean squared error (RMSE) is calculated as the following equation:

$$RMSE_m = \sqrt{\frac{\sum_t (Y_m(t) - U(x_m, t, \boldsymbol{k}))^2}{|t|}}\,.$$

The Table 3 shows that the RMSE of the computed values of the temperature with estimations is significantly lower than the *a priori* known values, except the $x_m = \{1, 10, 15\}$ cm. Consequently, in the most part of the region estimated values of the thermal diffusivities gives more accurate results than a priori known values.

Table 3. *RMSE between the measured and computed values of the temperature with estimations and a priori known values.*

x_m, cm	1	2	3	4	5	6	10	15	24	34	50
$RMSE_{est}$, $^\circ C$	0.7321	0.6344	0.1827	0.3606	0.3883	0.4953	0.5325	0.4595	0.3584	0.3096	0.1383
$RMSE_{apr}$, $^\circ C$	0.5801	0.6523	0.4534	0.7584	0.7747	0.9629	0.4830	0.4582	0.5599	0.5769	0.4449

3.4 Comparison of model predictions with additional data

The purpose of this section is to address the reliability of the mathematical model with the estimated parameters, by using measurements that were not considered for the inverse problem solution. As mentioned in Section 3.1, the inverse problem has been solved with measurements within $[0, 28]$ h, just before the rain events. Now, the reliability is addressed by also comparing measured and computed temperatures in $[28, 144]$ h, as shown by Figure 8. The rain events are marked by green dots in Figure 8. An analysis of these figures reveal that the proposed pure conduction model could also accurately predict the measurements at the points closer to the top surface, where the largest temperature variations took place. Note that the constant diffusivity proposed by the authors [19] provides acceptable results for the layers in depth higher than $x_m = 15$ cm.

The agreement between the computed temperatures and the measurements gets worse for sensors distant from the ground top surface. However, even at these deep positions the temperatures computed with the parameters after the solution of the inverse problem are in much better agreement with the measurements than the temperatures computed with the *a priori* known thermal diffusivity. Therefore, with the parameters estimated in this work, the proposed pure conduction model could appropriately predict the ground behavior even when discrete rain events took place.

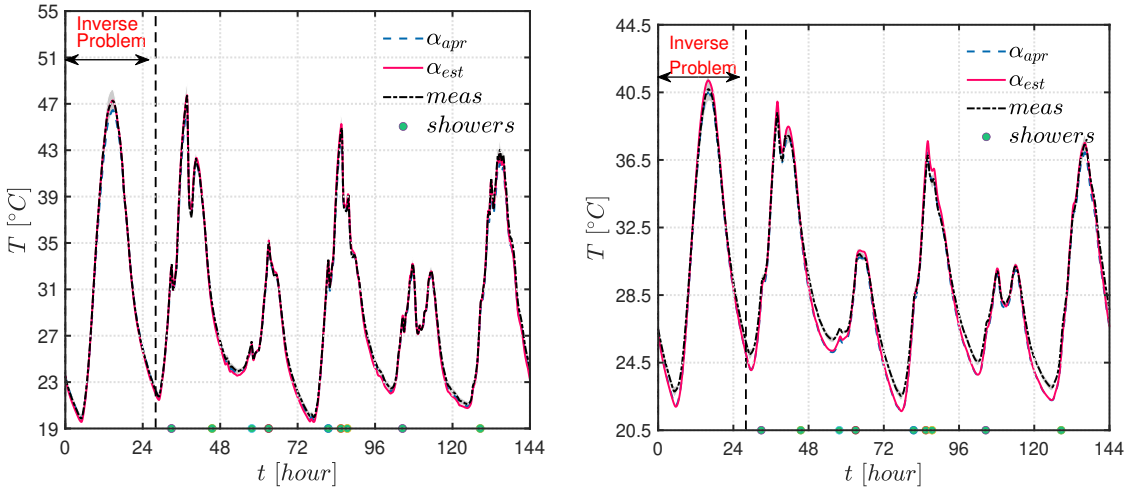

(a) $x_m = 3$ cm (b) $x_m = 10$ cm

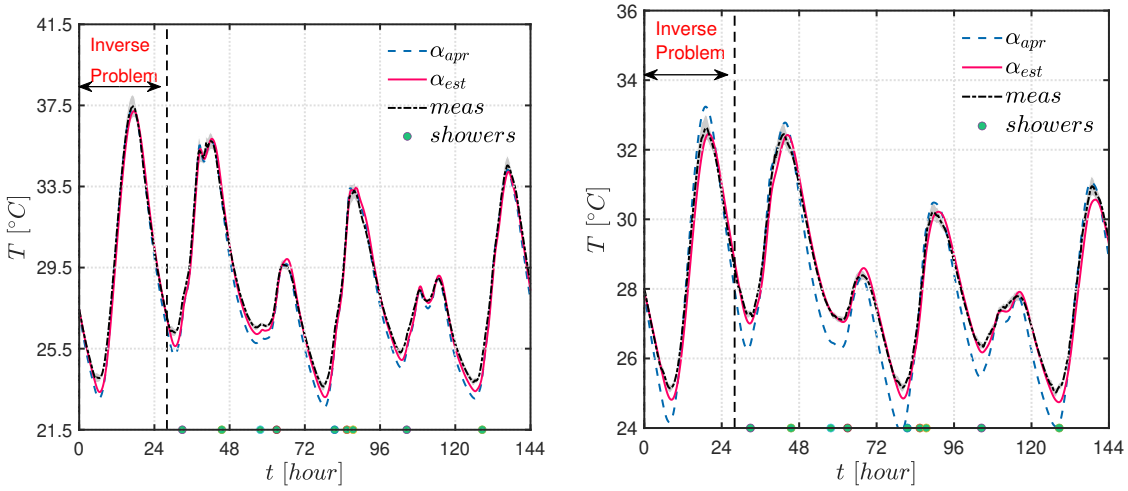

(c) $x_m = 15$ cm (d) $x_m = 24$ cm

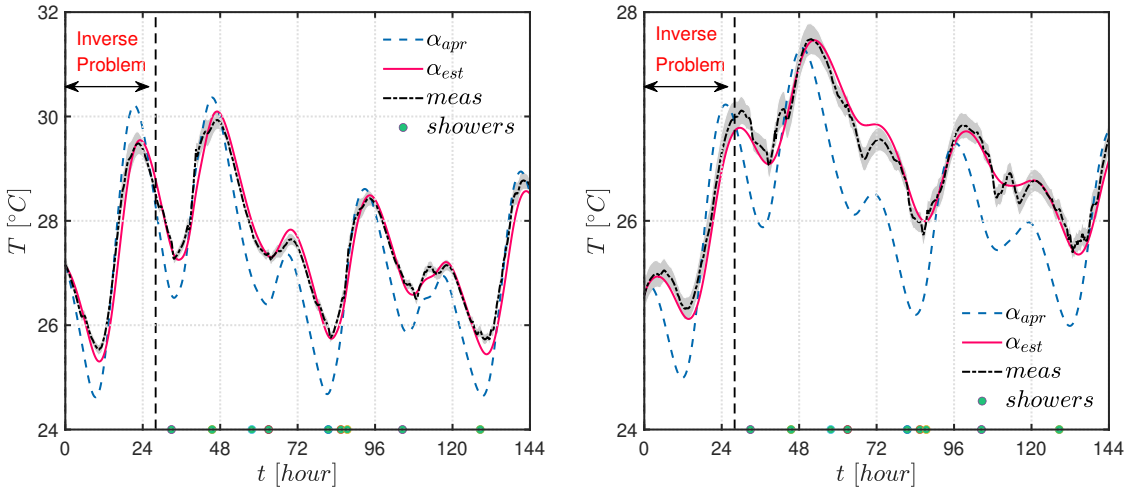

(e) $x_m = 34$ cm (f) $x_m = 50$ cm

Figure 8. *Evaluation of the model reliability by comparing predicted and measured temperature for the time interval* $[\,28\,,\,144\,]$ h .

4 Conclusion

In this paper, an inverse heat conduction problem was solved to indirectly measure thermal diffusivity spatial variation of an heterogeneous ground. The conjugate gradient method with adjoint problem formulation was applied for the solution of the inverse problem. Actual experimental data from a controlled experiment was used for the inverse analysis. The results obtained in this paper revealed that the applied method converged fast after only few iterations. However the discrepancy principle was not satisfied, but yet the estimated value of the thermal conductivity is better than the first study in the literature. Obtained values of thermal diffusivity were in agreement with values reported in the literature. The reliability of the calibrated model was also examined with measurements different from those used for the solution of the inverse problem. An overall good reliability was observed, with small discrepancies between computed and measured temperatures near the surface (around 1.6 $^{\circ}C$), where the ground behavior mostly interact with the surrounding environment and is most important for micro-climate predictions. Future works should focus on estimating other important parameters in the urban heat balance. Particularly, knowing precisely the thermal diffusivity of the ground, DIRICHLET boundary condition can be changed to Robin boundary condition to estimate the surface heat transfer coefficient and the solar absorptivity. The proposed methodology can be applied to determine such parameters that may vary with time (due to the wind velocity dependency). Moreover, having measured values of humidity, developed methodology can be extended for inverse heat and mass transfer problem to estimate ground moisture diffusivity.

Nomenclature

Latin letters		
c_ρ, c_0	specific heat capacity	$[\mathsf{J/(m^3.K)}]$
L	ground depth	$[\mathsf{m}]$
t_f	final time	$[\mathsf{s}]$
T	temperature	$[\mathsf{K}]$
t	time	$[\mathsf{s}]$
x	space coordinate	$[\mathsf{m}]$
U	dimensionless temperature	$[-]$
F_o	Fourier number	$[-]$
k	dimensionless heat conductivity	$[-]$

Greek letters		
κ	thermal conductivity	$[\mathsf{W/(m.K)}]$
α	thermal diffusivity	$[\mathsf{m^2/s}]$
ρ, ρ_0	density	$[\mathsf{kg/m^3}]$
σ_m	total standard deviation	$[^\circ C]$
σ_{meas}	measurement standard deviation	$[^\circ C]$
σ_{pos}	sensor location standard deviation	$[^\circ C]$
δ_x	sensor position uncertainty	$[\mathsf{m}]$

Subscripts and superscripts	
$*$	dimensionless parameter
apr	*a priori* parameter value
est	estimated parameter value

Acknowledgments

The authors acknowledge DSG 2021 project TOPS for the financial support. The authors thanks the grant AP19175447, AP19677594 from the Ministry of Science and Higher Education of the Republic of Kazakhstan. HRBO would like to acknowledge the financial support and hospitality of La Rochelle Université during his visit in May 2022.

References

[1] M. Kohler, C. Tannier, N. Blond, R. Aguejdad, and A. Clappier. Impacts of several urban-sprawl countermeasures on building (space heating) energy demands and urban heat island intensities. a case study. *Urban Climate*, 19:92–121, 2017. 1

[2] L.R. Rodríguez, J.S. Ramos, M.C.G. Delgado, and S.A. Domínguez. Implications of the urban heat island on the selection of optimal retrofitting strategies: A case study in a mediterranean climate. *Urban Climate*, 44:101234, 2022.

[3] T. Robineau, A. Rodler, B. Morille, D. Ramier, J. Sage, M. Musy, V. Graffin, and E. Berthier. Coupling hydrological and microclimate models to simulate evapotranspiration from urban green areas and air temperature at the district scale. *Urban Climate*, 44:101179, 2022.

[4] A. Bernabé, J. Bernard, M. Musy, H. Andrieu, E. Bocher, I. Calmet, P. Kéravec, and J. M. Rosant. Radiative and heat storage properties of the urban fabric derived from analysis of surface forms. *Urban Climate*, 12:205–218, 2015. 1

[5] L. Smalls-Mantey, K. DiGiovanni, M. Olson, and F.A. Montalto. Validation of two soil heat flux estimation techniques against observations made in an engineered urban green space. *Urban Climate*, 3:56–66, 2013. 1

[6] M. H. Azam, J. Bernard, B. Morille, M. Musy, and H. Andrieu. A pavement-watering thermal model for solene-microclimat: Development and evaluation. *Urban Climate*, 25:22–36, 2018.

[7] M. Musy, L. Malys, B. Morille, and C. Inard. The use of solene-microclimat model to assess adaptation strategies at the district scale. *Urban Climate*, 14:213–223, 2015. Cooling Heat Islands. 1

[8] M.H. Azam, J. Bernard, B. Morille, M. Musy, and H. Andrieu. A new urban soil model for solene-microclimat: Review, sensitivity analysis and validation on a car park. *Urban Climate*, 24:728–746, 2018. 1

[9] G. Hu, L. Zhao, X. Wu, R. Li, T. Wu, C. Xie, Y. Qiao, and G. Cheng. Comparison of different soil temperature algorithms in permafrost regions of qinghai-xizang (tibet) plateau of china. *Cold Regions Science and Technology*, 130:1–7, 2016. 1

[10] K. Malek, K. Malek, and F. Khanmohammadi. Response of soil thermal conductivity to various soil properties. *International Communications in Heat and Mass Transfer*, 127:105516, 2021. 1

[11] C. Liu, X. Hu, R. Yao, Y. Han, Y. Wang, W. He, H. Fan, and L. Du. Assessment of soil thermal conductivity based on bpnn optimized by genetic algorithm. *Advances in Civil Engineering, Hindawi*, 2020:105516, 2021. 1

[12] J. Berger, H. R.B. Orlande, N. Mendes, and S. Guernouti. Bayesian inference for estimating thermal properties of a historic building wall. *Building and Environment*, 106:327 – 339, 2016. 1

[13] J.V. Beck and K.J. Arnold. *Parameter estimation in engineering and science*. Wiley, 1977. 1, 6, 7

[14] P. J. Williams and M. W. Smith. *The frozen earth - fundamentals of geocryology*. Cambridge university press, 1991. 1

[15] R. Horton, P. J. Wierenga, and D. R. Nielsen. Evaluation of methods for determining the apparent thermal diffusivity of soil near the surface. *Soil Science Society of America Journal*, 47(1):25–32, 1983. 2

[16] S.V. Nerpin and A. F. Chudnovskii. *Physics of the soil*. Jerusalem: Keter Press, 1967. 2

[17] A.N. Kolmogorov. On the question of determining the coef cient of thermal diffusivity of the soil (in russian). *Izv. Acad. Sci. USSR. Geogr. Geophys.*, 2(14):97 – 99, 1950. 2

[18] J. Seemann. *Measuring Technology*, pages 40–45. Springer Berlin Heidelberg, Berlin, Heidelberg, 1979. 2

[19] J. M. Cohard, J.M. Rosant, F. Rodriguez, H. Andrieu, Mestayer P.G., and P. Guillevic. Energy and water budgets of asphalt concrete pavement under simulated rain events. *Urban Climate*, 24:675–691, 2018. 2, 8, 9, 13, 15

[20] F.A Rodrigues, H.R.B Orlande, and G.S Dulikravich. Simultaneous estimation of spatially dependent diffusion coefficient and source term in a nonlinear 1d diffusion problem. *Mathematics and Computers in Simulation*, 66(4):409–424, 2004. Inverse Obstacle Problems. 2

[21] M.J. Huntul, M.S. Hussein, D. Lesnic, M.I. Ivanchov, and N. Kinash. Reconstruction of an orthotropic thermal conductivity from non-local heat flux measurements. *International Journal of Mathematical Modelling and Numerical Optimisation*, 10(1):102 – 122, 2020.

[22] J. Santos, Y. Efendiev, and L. Guarracino. Hydraulic conductivity estimation in partially saturated soils using the adjoint method. *Computer Methods in Applied Mechanics and Engineering*, 196(1-3):161 – 179, 2006. 2

[23] N. Ukrainczyk. Thermal diffusivity estimation using numerical inverse solution for 1d heat conduction. *International Journal of Heat and Mass Transfer*, 52(25):5675–5681, 2009. 2

[24] K. Yang, T. Koike, B. Ye, and L. Bastidas. Inverse analysis of the role of soil vertical heterogeneity in controlling surface soil state and energy partition. *Journal of Geophysical Research D: Atmospheres*, 110(8):1 – 15, 2005. 2

[25] M. J. Colaco and H. R. B. Orlande. Comparison of different versions of the conjugate gradient method of function estimation. *Numerical Heat Transfer, Part A: Applications*, 36(2):229–249, 1999. 2

[26] H. Razzaghi, F. Kowsary, and M. Ashjaee. Derivation and application of the adjoint method for estimation of both spatially and temporally varying convective heat transfer coefficient. *Applied Thermal Engineering*, 154:63–75, 2019.

[27] K. Cao, D. Lesnic, and M. Colaco. Determination of thermal conductivity of inhomogeneous orthotropic materials from temperature measurements. *Inverse Problems in Science and Engineering*, 27, 11 2018.

[28] O. M. Alifanov. *Inverse heat transfer problems*. Springer Science & Business Media, 2012. 2, 5, 7

[29] O. Alifanov, E. Artyukhin, and S. Rumyantsev. *Extreme Methods for Solving Ill-Posed Problems with Applications to Inverse Heat Transfer Problems*. Begell House, inc. New York - Wallingford (U.K.), 04 2015. 2, 7

[30] M.N. Ozisik and H.R.B. Orlande. *Inverse Heat Transfer - Fundamentals and Applications*. CRC Press, New York, 2000.

[31] H.R.B. Orlande, O. Fudym, D. Maillet, and R.M. Cotta. *Thermal Measurements and Inverse Techniques*. Heat Transfer. CRC Press, 2011. 2, 5, 6, 7

[32] E. Polak. *Computational Methods In Optimization*. Academic Press, New York, 1985. 6

[33] J. E. Dennis and R. B. Schnabel. *Numerical Methods for Unconstrained Optimization and Nonlinear Equations*. Society for Industrial and Applied Mathematics, 1996. 7

[34] A. Verhoef, B. Hurk, A. Jacobs, and B.G. Heusinkveld. Thermal soil properties for a vineyard (efeda-i) and savanna (hapex-sahel) sites. *Agricultural and Forest Meteorology*, 78:1–18, 1996. 8

[35] F.P. Incropera, D.P. DeWitt, T.L. Bergman, and A.S. Lavine. *Fundamentals of Heat and Mass Transfer*. John Wiley and Sons, England, 6 edition, 2006. 8, 12, 13

[36] J.R. Taylor. *Introduction To Error Analysis: The Study of Uncertainties in Physical Measurements*. ASMSU/Spartans.4.Spartans Textbook. University Science Books, 1997. 8

[37] D. Ucinski. *Optimal Measurement Methods for Distributed Parameter System Identification*. CRC Press, 2004. 9

[38] S. Gasparin, J. Berger, D. Dutykh, and N. Mendes. An improved explicit scheme for whole-building hygrothermal simulation. *Building Simulation*, 11(3):465–481, 2018. 9

[39] A. Kavianipour and J.V. Beck. Thermal property estimation utilizing the laplace transform with application to asphaltic pavement. *International journal of heat and mass transfer*, 20(3):259–267, 1977. 12, 13

[40] J. M. A. Marquez, M. A. M. Bohorquez, and S. G. Melgar. Ground thermal diffusivity calculation by direct soil temperature measurement. application to very low enthalpy geothermal energy systems. *Sensors*, 16(3), 2016. 12, 13

[41] Q. Xu and M. Solaimanian. Modeling temperature distribution and thermal property of asphalt concrete for laboratory testing applications. *Construction and building materials*, 24(4):487–497, 2010. 13